Continuous wave phase detection for probing nonlinear elastic wave interactions in rocks

Paul A. Johnson
Earth and Environmental Sciences Divisions, Mail Stop D443, Los Alamos National Laboratory, Los Alamos, New Mexico 87545

Albert Migliori
Physics Division, Mail Stop K764, Los Alamos National Laboratory, Los Alamos, New Mexico 87545

Thomas J. Shankland
Earth and Environmental Sciences Division, Mail Stop D447, Los Alamos National Laboratory, Los Alamos, New Mexico 87545

(Received 16 May 1990; accepted for publication 18 September 1990)

A new method that uses nonlinear elastic wave generation to produce a continuous wave (cw) phase measurement from which dimensions or velocities of a body can be obtained is described. Like the technique of standing wave resonance for obtaining sound velocities, this method takes advantage of the high accuracy characteristic of frequency measurements. In the experiment, two intersecting, high-frequency primary signals f_1 and f_2 are mixed inside a sample, creating a directional beam at the difference frequency $\Delta f = f_1 - f_2$. An externally generated, low-pass-filtered Δf signal is electronically mixed with the signal obtained from the sample. As either primary frequency is swept, the dc component from the mixer varies between relative maximum and minimum values at characteristic frequency intervals depending on the phase differences. The resulting interference signal can be used to calculate the distance from the mixing volume in the sample to the detector and to the two primary signal transmitters, providing that a single characteristic distance and wave velocities are known. The reverse experiment is determining velocities from known dimensions.

PACS numbers: 43.25. Zx

INTRODUCTION

Nonlinear elastic wave interactions can be used in unique ways to obtain physical properties of materials. The study of nonlinear acoustics shares general analogies with nonlinear optics or with nonlinear devices in electronics in that a variety of frequency shifting and interference effects become possible. Thus an early interest in underwater acoustics[1] was in beating collinear, high-frequency beams to produce a collimated beam at the lower, and less attenuated, difference frequency. We have similar goals of developing a difference frequency signal source for use in the earth and of understanding physical properties of earth materials, although the methods given here could be applied to any solid.

This work on nonlinear elasticity differs from previous efforts in two ways. First, this paper shows how elastic waves generated within a material can be made to interfere and then be mixed with an externally generated signal to precisely determine elastic properties of a solid. Second, the samples are rocks, which are fractured rather than intact materials. Rocks, like many ceramics, contain a fine network of microfractures; as these cracks close with applied stress, there are large changes in elastic moduli.[2] The change in a modulus M with pressure P, dM/dP, can be nearly two orders of magnitude larger in rocks than in an uncracked material such as a liquid or crystal. Nonlinear conversion efficiency from primary to difference frequency beams increases with dM/dP and is higher than within uncracked materials (on the order of a percent[3]). However, the enhanced nonlinear conversion is partially diminished by the larger elastic wave attenuation generally characteristic of rocks.

Mixing of high-strain-amplitude primary waves f_1 and f_2 in a manner that produces a difference frequency beam results from conservation of energy and momentum, and is described by selection rules derived from nonlinear elastic wave theory.[3,4] In the case of intersecting primary beams, when a particular frequency ratio f_2/f_1 is chosen and a ratio of shear to compressional wave velocity v_s/v_p given by the material, the mixing angle ϕ between primary signals and the take-off angle θ of the scattered beam are fixed. Alternatively, when either angle is chosen, the second angle and frequency ratio are fixed. Figure 1 illustrates the relationships for wave vector $\mathbf{k}$ that result from conservation of momentum. Figure 2 shows the relationship between angles and propagation paths L_i. Note that the triangle of Fig. 1(b) is not in general similar to that of Fig. 2; the first is in wave-vector space and the second is in cartesian space.

Earlier experiments verified that nonlinear interactions of elastic waves indeed take place in rocks. This work demonstrated that nonlinear mixing of two intersecting, high-frequency signals f_1 and f_2 inside a rock sample produced a scattered beam at the difference frequency Δf.[5] Verification was accomplished by demonstrating that frequency and angular relationships between the primary and difference fre-

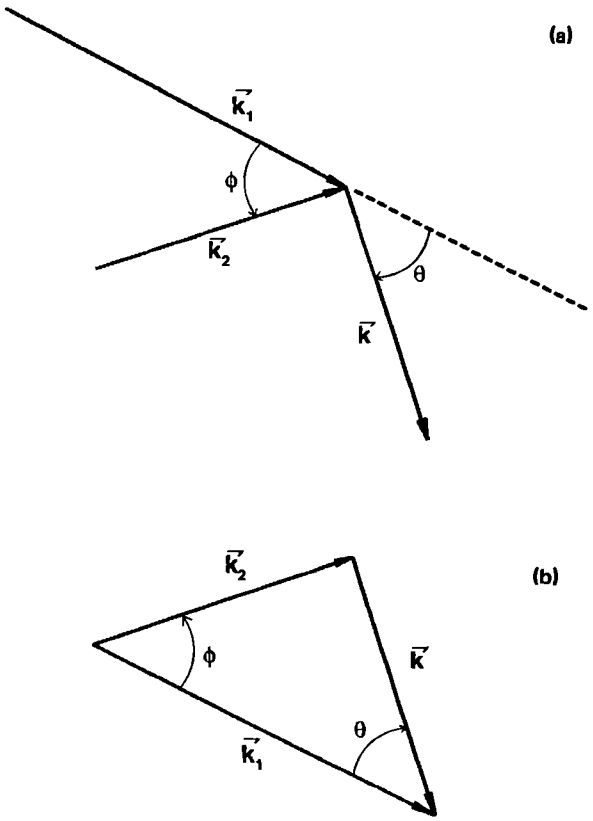

FIG. 1. (a) The k-vector relationship between primary signals and the difference frequency beam. (b) k-vector subtraction.

quency signals obeyed selection rules derived from nonlinear elastic wave theory.[3,4] We later used pulsed-mode signals to show that total transit times of primary plus difference frequency signals matched their predicted values, providing further evidence that nonlinear mixing was taking place inside the material.[6]

There are two interaction cases that produce a difference frequency in the case of intersecting (noncollinear) primary signals, as described by the selection rules.[3,4] Two compressional waves can interact to produce a shear wave polarized in the plane created by the primary wave vectors. Alternatively, a shear wave, also polarized in the plane formed by the wave vectors, and a compressional wave can interact to create another compressional wave. We will treat the former case.

This paper discusses a continuous wave (cw) method using the nonlinearly generated beam by measuring the phase of the received signal. In the cw method, data are collected over the entire duration of an experiment, as opposed to pulsed-mode techniques where signals are present only for brief time intervals. The higher duty cycle of the cw method produces equivalent information in a shorter period of time. The cw method is applied to determining wave propagation distances because determining distances in a rock body is a basic problem in underground imaging. An equivalent problem, which is the usual laboratory one, is obtaining wave transit times when characteristic distances are known. Measuring transit time of the difference frequency beam in the time domain is difficult, however, because direct arrivals of the primary signals traveling over a shorter path can overlap with the arrival of the difference frequency beam at the detector. Extracting the small amplitude, difference frequency signal from the larger amplitude primary arrivals requires fairly extensive signal processing.[6] The new method presented here for obtaining wave propagation path lengths avoids this problem altogether. In the following, we describe the laboratory apparatus, mathematical theory, and experimental results for the new method. We then discuss the advantages of the method in terms of accuracy of calculated propagation path lengths and transit time measurements.

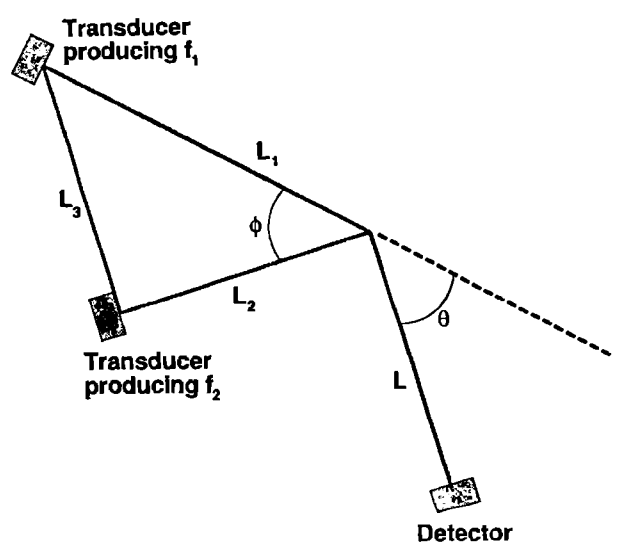

FIG. 2. Geometry of interaction. Note that the triangle in this figure is not necessarily identical to that of Fig. 1(b), which is in wave-vector space.

I. EXPERIMENTAL METHOD AND APPARATUS

As previously noted, two significant problems related to signal-to-noise ratio arise when measuring transit time using pulsed-mode methods. These are: (1) In the case of intersecting signals where a difference frequency created by nonlinear mixing is to be measured, the detected signal is complicated in that it is composed of the superposition of primary signals and the difference frequency signal that all overlap in time; and (2) the signal-to-noise ratio of the difference frequency signal is diminished because of the combined effects from low conversion efficiency, elastic wave attenuation, and broadband electronics. Little or nothing can be done to eliminate the problem of signals overlapping in time at the detector, nor to diminish the effects of attenuation. Within the limits imposed by the electronics, conversion efficiency can be improved somewhat by increasing the voltage applied to the primary signals f_1 and f_2 up to a maximum where acoustic saturation takes place.[7] Signal-to-noise ratio can be improved somewhat by signal averaging. How-

ever, the necessarily low duty cycle of pulsed measurements (typically $<0.1\%$) is inefficient: much of the measurement time consists of waiting, and only briefly is there is a signal present. Increasing the repetition rate and thus the duty cycle is often limited by reverberations within the sample and by the transducers and electronics. Furthermore, obtaining an accurate arrival time requires accurate timing, which in turn requires wideband electronics; using wideband electronics generally decreases signal-to-noise ratio. Limiting bandwidth with band-pass filters only reduces timing accuracy.

Continuous wave phase measurements can provide improved signal-to-noise ratio and decreased data collection time as compared to pulsed-mode measurements. In the linear case of a single source exciting resonant mode standing waves in a sample of know physical dimensions, velocity is calculated from the frequency interval δf between observed adjacent resonant peak amplitudes as frequency is swept from one peak to the next. The interval δf is equivalent to a phase shift, which in turn can be related to transit time and path length. Using cw phase measurements provides a significant increase in signal-to-noise ratio for the same real time because the duty cycle is increased to 100%, effectively increasing N, the number of signals summed and averaged. Furthermore, measuring frequency rather than time permits narrow bandwidth detection, which allows selective band-pass filtering to enhance signal-to-noise ratio in addition to providing the inherent high accuracy afforded by frequency generation.

We have developed a method analogous to the single-source-generated standing waves. In this more general scheme, we obtain wave propagation lengths by measuring the phase difference between the nonlinearly derived difference frequency wave produced in a rock sample and an electronically derived difference frequency obtained by multiplicative mixing of the primary signals.

Figure 3 is a block diagram of the experimental apparatus. Frequencies f_1 and f_2 are provided by two separate function generators to two compressional wave source transducers and also to a high-frequency, low-noise mixer (multiplier), denoted "first mixer" in the figure. The mixer output is the product of the two drive signals, which can be expressed as a superposition of the sum and difference frequencies. A low-pass filter attenuates f_1+f_2 from the mixer output and any leakage of the primaries f_1, f_2, leaving the difference frequency $\Delta f=f_1-f_2$. This electronically produced difference frequency signal is then fed to a second mixer. The other input to the second mixer is the amplified signal output from nonlinear mixing of waves in the sample, also low-pass filtered. The output of the second mixer contains a dc level that depends on the phase delay between the two input difference frequency signals. Since the dc component is the signal of interest in the phase measurement, any remaining higher-frequency contamination can be removed by another low-pass filter. As one of the primary frequencies is swept, the dc level oscillates with the interfering phase relationships between the electronic and elastic wave difference frequencies. We can narrow-band detect variations of this dc signal with a half-second time constant (the response time for the dual slope integrating digital voltmeter, HP3457A) as a primary frequency is swept, thus providing an impressively narrow 2-Hz bandwidth for the detection of 200–700-kHz difference frequencies. Narrow-band detection produces further signal-to-noise increase. By sweeping f_1 or f_2, we obtain the dc phase relationship intervals necessary for extracting wave propagation distances.[8]

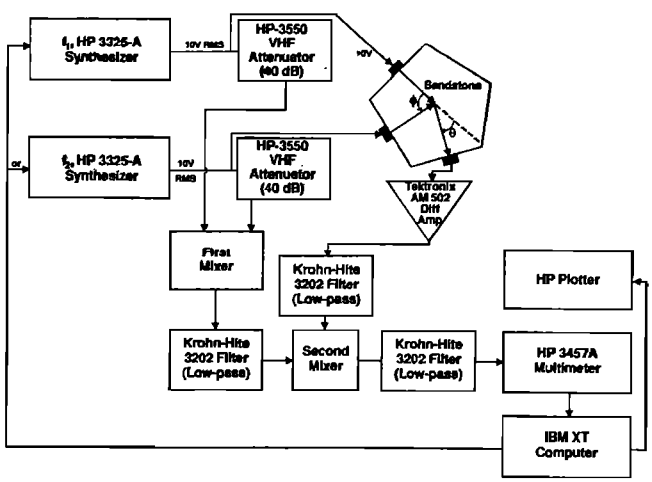

FIG. 3. Experimental configuration.

II. THEORY

The interference conditions can be demonstrated in the following theoretical result. The signals used to drive the two source transducers $A_1\sin(\omega_1 t)$ and $A_2\sin(\omega_2 t)$ combine in an electronic mixer to produce a voltage given by

$$V(t)=A_1\sin(\omega_1 t)A_2\sin(\omega_2 t),$$

that can be represented as a sum and difference frequency term. Here, $V(t)$ is the voltage of the mixed signal, A_1 and A_2 are the amplitudes of the input signals, ω_1 and ω_2 are angular frequencies $2\pi f_1$ and $2\pi f_2$, respectively, and phase is arbitrarily taken to be zero. Low-pass filtering eliminates the sum frequency term from the electronically mixed signal, leaving

$$V(t)=(A_1A_2/2)\cos[(\omega_1-\omega_2)t]. \quad (1)$$

The two primary waves in the rock are $P_1\sin(\omega_1 t-k_1L_1)$ and $P_2\sin(\omega_2 t-k_2L_2)$, where P_1 and P_2 are amplitudes, k_1 and k_2 are wave numbers ($k_i=\omega_i/v_p$), and L_1 and L_2 are distances of travel from the drivers to the mixing region shown in Fig. 2. Nonlinear mixing in the rock produces the product (that can also be represented by sum and difference frequencies)

$$P(t)=P_1\sin(\omega_1 t-k_1L_1)P_2\sin(\omega_2 t-k_2L_2).$$

After propagation to the detector, the signal is low-pass filtered to reduce the two primary frequencies and the sum frequency, leaving

$$P_d(t) = R(P_1P_2/2)\cos[(\omega_1 - \omega_2)t - kL - k_1L_1 + k_2L_2], \quad (2)$$

where R includes effects of attenuation, spreading, and scattering, $k = \omega/v_s$, L is the distance from the interaction region to the detector, and $P_d(t)$ is the voltage of the difference frequency beam. On combining (1) and (2) in the second mixer we have

$$V_{\text{out}}(t) = 2B\cos(\omega_1 - \omega_2)t \times\cos[(\omega_1 - \omega_2)t - kL - k_1L_1 + k_2L_2],$$

where $2B = RP_1P_2A_1A_2$, and $V_{\text{out}}(t)$ is the measured output voltage. From the time average and after low-pass filtering, there remains a residual dc signal of the form

$$V_{\text{out}}(t) = B\cos(kL + k_1L_1 - k_2L_2). \quad (3)$$

Defining the velocity ratio $\alpha = v_s/v_p$ we can write

$$k = (\omega_1 - \omega_2)/\alpha v_p,$$
$$k_1 = \omega_1/v_p,$$
$$k_2 = \omega_2/v_p,$$

and (3) becomes

$$V_{\text{out}}(t) = B\cos\{(2\pi/v_p)[(f_1 - f_2)L/\alpha + f_1L_1 - f_2L_2]\}.$$

The phase condition to produce maximum V_{out} is

$$(f_1 - f_2)L/\alpha + f_1L_1 - f_2L_2 = nv_p, \quad (4)$$

where n is an integer related to the total number of wavelengths between sources and receiver. When f_1 is swept upward in frequency by δf_1 so that the dc signal advances from the nth peak to the (nth + 1) peak (where the two difference frequencies are again in phase), (4) becomes

$$(f_1 + \delta f_1 - f_2)L/\alpha + (f_1 + \delta f_1)L_1 - f_2L_2 = (n+1)v_p, \quad (5)$$

where δf_1 is the characteristic frequency interval between peaks of the difference frequency when f_1 is swept. On sweeping f_2 downward in frequency by δf_2 so that the dc signal advances from the nth peak to the (nth + 1) peak (4) becomes

$$[f_1 - (f_2 - \delta f_2)]L/\alpha + f_1L_1 - (f_2 - \delta f_2)L_2 = (n+1)v_p, \quad (6)$$

where δf_2 is the characteristic frequency interval between peaks of the difference frequency as f_2 is swept. (note that $f_1 - f_2$ increases as f_2 decreases and thus n *increases* in this case. Also, δf_1 and δf_2 are in general *not the same* but depend on f_1 and f_2, respectively.) Subtracting (4) from (5) and (6), respectively, yields

$$L/\alpha + L_1 = v_p/\delta f_1, \quad (7)$$
$$L/\alpha + L_2 = v_p/\delta f_2. \quad (8)$$

From the geometry illustrating interaction angles and lengths shown in Fig. 2, the law of cosines gives

$$L_3^2 = L_1^2 + L_2^2 - 2L_1L_2\cos(\phi). \quad (9)$$

Since L_3 can be measured directly as the distance between centerlines of the driving transducers, (7),(8), and (9) represent three equations and three unknowns, which can be solved exactly for the lengths L, L_1, and L_2. Transit times equivalent to those measured by pulsed techniques could be readily obtained from these calculated lengths and known velocities.

III. EXPERIMENT

The sample was a sandstone from Berea, Ohio, a standard material for many experiments in rock physics. It was cut for specific angles ϕ and θ, which were calculated from the selection rules for the measured average v_s/v_p of 0.64. The frequency ratio f_2/f_1 for maximum response at Δf was arbitrarily chosen to be 0.61 and thus the angles ϕ and θ were fixed at 34° and 34.5°, respectively.[6] Frequency ratio, angles, and velocities are compiled in Table I. An initial measurement was taken by first sweeping primary frequency f_1 over a broad frequency range for gross characterization of the dc signal at fixed f_2; the sweep was repeated with a finer frequency step to measure the characteristic frequency interval δf_1 between peaks. A measurement was then taken by sweeping f_2 with f_1 fixed in order to obtain δf_2. In each case, dc voltage was plotted versus frequency, and the characteristic frequency interval δf_i was obtained from these plots. Frequency sweeps and data storage were controlled by the computer. A single sweep experiment took 1–2 min.

IV. RESULTS

Figure 4 illustrates output from the multimeter obtained by sweeping f_1 from 500–620 kHz with f_2 fixed at 366 kHz. The inset shows the overall pattern of the signal when f_1 was swept from 475–725 kHz. Note that the frequency increments of f_1 used in the fine and gross characterization are 0.5 and 10 kHz, respectively; thus shapes of the curves do not match identically. The higher resolution plot was used

TABLE I. Physical parameters and geometrical relationships of sandstone sample. The distances for L_1, L_2, and L were determined both from the phase measurement (P) and by direct measurement (D) using a ruler on the surface of the rock.

Frequency ratio	ϕ (deg)	θ (deg)	Average velocity v_p (km/s)	Average velocity v_s (km/s)	Average velocity ratio	L_1 (mm)	L_2 (mm)	L_3 (mm)	L (mm)	
0.61	34	34.5	2.78	1.77	0.64	93	89		74	(P)
						93	91	55	77	(D)

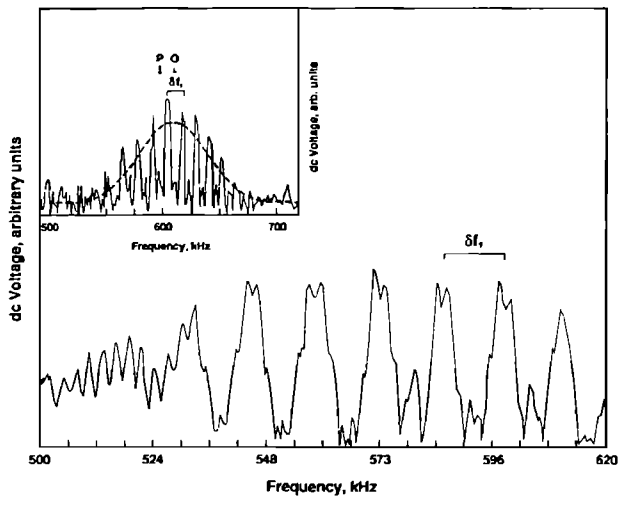

FIG. 4. Plot of dc voltage versus frequency, where f_1 was swept from 500–620 kHz and f_2 was fixed at 366 kHz. The measured characteristic frequency interval δf_1 was 13.3 kHz. The inset shows a larger frequency sweep interval curve to illustrate the shape of the low-frequency envelope (dashed line through data). Observed (O) and predicted (P) peaks are very similar (arrow).

for the actual measurement of δf_1. The interval δf_1 measured between peaks was 13.3 kHz, obtained by averaging over several peaks in the higher resolution plot. Figure 5 illustrates the result when f_1 was fixed at 600 kHz and f_2 was swept from 200–400 kHz. In this case, the interval δf_2 was measured to be 13.6 kHz. The inset is an expanded sweep of f_2 from 250–500 kHz.

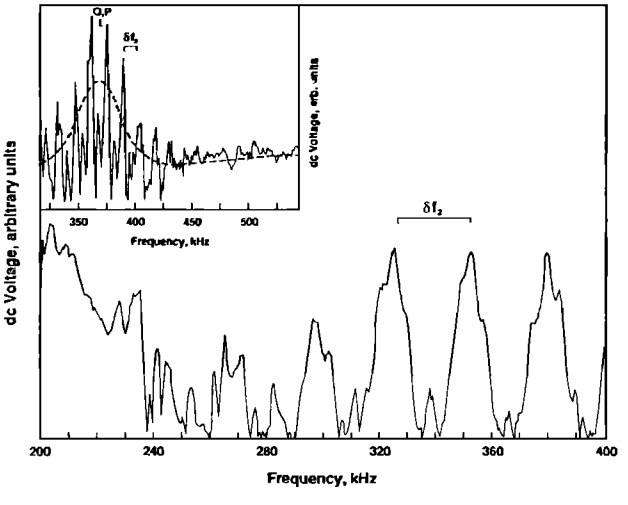

FIG. 5. Plot of dc voltage versus frequency, where f_2 was swept from 200–400 kHz and f_1 was fixed at 600 kHz. Measured characteristic frequency interval δf_2 was 13.6 kHz. Inset: Low-frequency shape of data shown by dashed line. Observed and predicted peaks are equal to within experimental error (arrow).

Substitution of $\delta f_1 = 13.3$ kHz and $\delta f_2 = 13.6$ kHz into (7),(8), and (9) together with the necessary velocities, angles, and L_3 from Table I, yields the distances of propagation from the sources to the center of the mixing region and from the mixing region to the detector. Here, L_1,L_2, and L were calculated to be 93,89, and 74 mm, respectively. These values are within 2.2% of the measured lengths (Table I).

A combined transit time was calculated by summing the transit times along propagation paths L_1 and L by using L_1 and L from the interference experiment and v_p and v_s, respectively. The calculated total transit time is 75.3 μs, as compared to 73 μs obtained from a pulsed-mode measurement.[6] In light of the velocity anisotropy of 6%–7%, the agreement is quite good.

The interference curves contain information about wave propagation paths and are therefore a demonstration that nonlinear mixing of the primary beams takes place in the sample. They also contain an independent verification of the mixing phenomenon in the rock in the envelope of the dc output, shown by the dashed line in the insets of Figs. 4 and 5. According to the selection rules, the peak amplitude of the envelope of the dc signal should occur at $f_2/f_1 = 0.61$ for angles $\phi = 34°$ and $\theta = 34.5°$. The ratio should occur at $f_1 = 600$ kHz (P in the inset of Fig. 4) when f_2 is fixed at 366 kHz. The observed peak in the envelope occurred at approximately 605 kHz (O in Fig. 4), within 0.8% of the predicted value. Similarly, the envelope peak should occur at $f_2 = 366$ kHz when f_1 is fixed at 600 kHz, as shown in the inset of Fig. 5; in this case, the peak values, estimated by eye, appeared to be identical. Note that, if mixing occurred only in the electronics, neither the low-frequency envelope, nor δf_1 and δf_2 would be produced.[3,5]

V. DISCUSSION

It is seen that propagation distances into and away from the center of the mixing region determined by the cw phase method can be calculated to within a few percent. This accuracy is remarkably good when it is considered that the driver transducers are 25 mm in diameter and the interaction volume has even greater length and width. The measurement depends on distance of separation between primary transducers, interaction angles between the primary signals and the difference frequency signal, and on the phase difference between the electronically mixed difference frequency signal and the physically mixed difference frequency signal. The distance between the centers of the primary transducers can be readily measured directly from the rock sample to within 2 mm, about 2% of the distance. The angle between transducers is fixed arbitrarily by the test configuration and depends on how accurately the transducers are placed. This error is less than 0.5°. In addition, the large signal-to-noise ratio resulting from the cw mode measurement allows us to measure the frequency intervals to within 100 Hz.

As mentioned earlier, rocks are elastically anisotropic, and in this specimen, sound velocities in different directions differ by a total of 6%–7%. Effects of anisotropy could include leakage into different modes and possible beam broadening. An example of mode leakage might be a primary shear-wave beam oriented off a principal axis, producing

shear-wave splitting. This could result in diminished primary and difference frequency wave amplitudes. Although broadened primary beams have a large interaction volume, hence higher intensities at the difference frequency, the general consequence is expected to be a broadened difference frequency signal and a slight degradation of accuracy in angle measurements. Furthermore, the broadened difference frequency signal may slightly decrease the expected signal-to-noise ratio predicted for a more directed beam.

The procedure in these experiments has been to treat as known the velocities v_p and v_s, distance L_3, and angle ϕ between transducers. When the frequency ratio f_2/f_1 is chosen, the angles ϕ and θ for signal intersection and emission are determined by the nonlinear selection rules. This leaves the distances L_1, L_2, and L to the center of the interaction region to be obtained from the experiment. There are circumstances underground where such information would be helpful, e.g., imaging large fractures or other changes in acoustic impedance. Ordinarily, in geophysical problems, distances would be measured from transit times of elastic waves, providing velocities are known. Alternatively, if we knew distances, then we could calculate v_p and v_s, but this procedure might require some iteration to optimize interaction angles to match the nonlinear selection rules.

Finally, advantages over conventional ultrasonic methods include enhanced signal-to-noise ratio and therefore superior measurement accuracy, in decreased data collection time. A further advantage is the ability to steer the difference frequency beam. Disadvantages of this method include the additional components required in configuring the experiment, including the requirement of the mixers described previously. Geometrical constraints imposed by the selection rules produce an additional difficulty, as does the signal measurement, i.e., determining the oscillation frequency of the interference signal as compared to measuring a travel time directly.

VI. CONCLUSIONS

The cw nonlinear interference method takes advantage of nonlinear elastic properties to determine wave propagation distances across a material. The method resembles standard elastic wave resonance techniques developed for measuring velocities in various materials by measuring phase differences. We have extended the technique by including nonlinear wave generation and then measuring phase differences to calculate propagation distances when velocities are given. Propagation distances to the center of the interaction region obtained from phase measurements agree with measured distances to about 2.2%. The reverse application of the method is to obtain velocities when dimensions are known. The quality of the distance measurements indicates that possible measurements of velocities could be obtained to good accuracy.

ACKNOWLEDGMENTS

We are indebted to Peter Roberts and Leigh House for thorough reviews of the manuscript. This work was performed under the auspices of the Office of Basic Energy Research, U. S. Department of Energy under Contract No. W-7405-ENG-36 with the University of California.

[1] P. Westervelt, "Parametric acoustic array," J. Acoust. Soc. Am. **35**, 535–537 (1963).

[2] K. W. Winkler, A. Nur, and M. Gladwin, "Friction and seismic attenuation in rocks," Nature **277**, 528–531 (1979).

[3] L. H. Taylor and F. R. Rollins, Jr., "Ultrasonic study of three-phonon interactions, I, Theory," Phys. Rev. **136**, A591–A596 (1964).

[4] G. L. Jones and D. Kobett, "Interaction of elastic waves in an isotropic solid," J. Acoust. Soc. Am. **35**, 5–10 (1963).

[5] P. A. Johnson, T. J. Shankland, R. J. O'Connell, and J. N. Albright, "Nonlinear generation of elastic waves in crystalline rock," J. Geophys. Res. **92**, 3597–3602 (1987).

[6] P. A. Johnson and T. J. Shankland, "Nonlinear generation of elastic waves in granite and sandstone: Continuous wave and travel time observations," J. Geophys. Res. **94**, 17727–17733 (1989).

[7] T. G. Muir, "Nonlinear acoustics: A new dimension in underwater sound," in *Science, Technology and the Modern Navy, 30th Anniversary 1946–1976*, edited by E. I. Salkovitz (Department of the Navy, Office of Naval Research, Arlington, VA, 1976), pp. 548–569.

[8] The measurement relies on the low-noise, high-frequency mixers (multipliers) designed and constructed by us. The schematics are available on request from the authors.